JOURNAL OF GEOPHYSICAL RESEARCH, VOL. 101, NO. E2, PAGES 4623–4635, FEBRUARY 25, 1996

Laboratory measurement of the temperature dependence of gaseous sulfur dioxide (SO_2) microwave absorption with application to the Venus atmosphere

Shady H. Suleiman
School of Electrical and Computer Engineering, Georgia Institute of Technology, Atlanta

Marc A. Kolodner
School of Physics, Georgia Institute of Technology, Atlanta

Paul G. Steffes
School of Electrical and Computer Engineering, Georgia Institute of Technology, Atlanta

Abstract. High-accuracy laboratory measurements of the temperature dependence of the opacity from gaseous sulfur dioxide (SO_2) in a carbon dioxide (CO_2) atmosphere at temperatures from 290 to 505 K and at pressures from 1 to 4 atm have been conducted at frequencies of 2.25 GHz (13.3 cm), 8.5 GHz (3.5 cm), and 21.7 GHz (1.4 cm). Based on these absorptivity measurements, a Ben-Reuven (BR) line shape model has been developed that provides a more accurate characterization of the microwave absorption of gaseous SO_2 in the Venus atmosphere as compared with other formalisms. The developed BR formalism is incorporated into a radiative transfer model. The resulting microwave emission spectrum of Venus is then used to set an upper limit on the disk-averaged abundance of gaseous SO_2 below the main cloud layer. It is found that gaseous SO_2 has an upper limit of 150 ppm, which compares well with previous spacecraft in situ measurements and Earth-based radio astronomical observations.

1. Introduction

Laboratory measurements of the microwave absorbing properties of gaseous sulfur dioxide (SO_2) under simulated conditions for the Venus atmosphere are necessary for the interpretation of radio absorptivity data obtained from spacecraft radio occultation experiments and Earth-based radio astronomical observations. In the past, laboratory measurements have been conducted to characterise the microwave and millimeter-wave opacity of gaseous SO_2 under Venus-like conditions. *Steffes and Eshleman* [1981] concluded that at pressures from 1 to 5 atmospheres (atm) and at temperatures from 297 to 355 Kelvin (K) that the absorption coefficient of gaseous SO_2 in a carbon dioxide (CO_2) atmosphere at 2.257 and 8.342 GHs had a f^2 frequency dependence and was approximately 50% larger than that computed from the Van Vleck-Weisskopf (VVW) line shape theory. However, their preliminary measurements did not account for the effects of "dielectric loading" in the resonator used for the experiment [*see Spilker*, 1993]. Subsequently, *Fahd and Steffes* [1992] conducted absorptivity measurements of gaseous SO_2 in a CO_2 atmosphere at room temperature (296 K) which partially took into account the effects of dielectric loading for the following frequencies (wavelengths): 2.24 GHs (13.3 cm), 21.7 GHs (1.32 cm), and 94.1 GHs (0.32 cm). These measurements showed that the absorption coefficient of gaseous SO_2 in a CO_2 atmosphere is in agreement with the VVW line shape theory at 21.7 and 94.1 GHs but not at 2.24 GHs. In addition, the results showed that the f^2 frequency dependence of the opacity of gaseous SO_2 is not uniformly valid for all frequencies below 100 GHs and pressures above 1 atm. Although some preliminary laboratory measurements of the opacity of gaseous SO_2 in a CO_2 atmosphere in the temperature range from 297 to 355 K were made at 2.257 and 8.342 GHs [*Steffes and Eshleman*, 1981], no measurements of the temperature dependence of gaseous SO_2 opacity were made for higher frequencies or temperatures. As a result, high-accuracy laboratory measurements of the temperature dependence of the opacity from gaseous SO_2 in a CO_2 atmosphere at characteristic temperatures of the Venus atmosphere are of significance. These measurements can provide more accurate abundance estimates of gaseous SO_2 in the atmosphere of Venus.

This paper describes the methodology and the results of the laboratory measurement of the temperature dependence of the opacity from gaseous SO_2 in a CO_2

Paper number 95JE03728.
0148-0227/96/95JE-03728$05.00

atmosphere at temperatures from 290 to 505 K and at pressures from 1 to 4 atm for the following frequencies (wavelengths): 2.25 GHz (13.3 cm), 8.5 GHz (3.5 cm), and 21.7 GHz (1.4 cm). Based on these absorptivity measurements, this paper presents a new Ben-Reuven (BR) line shape model that provides a more accurate characterisation of the microwave absorption of gaseous SO_2 in the Venus atmosphere as compared with other formalisms. Finally, the developed BR formalism is incorporated into a radiative transfer model, and the resulting microwave emission spectrum of Venus is then used to infer an upper limit on the disk-averaged abundance of gaseous SO_2 below the main cloud layer.

2. Method of Measurement

2.1. Experimental Approach

For a relatively low loss gaseous mixture, the absorption coefficient or attenuation constant α, which is defined as the power loss per unit length, is given by [e.g., *Ramo et al.*, 1965]

$$\alpha \cong \frac{\pi}{\lambda}\frac{\epsilon''}{\epsilon'} = \frac{\pi}{\lambda}\frac{1}{Q_g}, \tag{1}$$

where ϵ' and ϵ'' are the real and imaginary parts of the complex permittivity $\epsilon = \epsilon' - j\epsilon''$, and $Q_g = \epsilon'/\epsilon''$ is the quality factor of the low-loss gaseous mixture. Thus, to measure α at wavelength λ, Q_g should be known. In general, Q_g can be measured by introducing the gaseous mixture into a cavity resonator and observing its effect on the resonant properties of the cavity [e.g., *Townes and Schawlow*, 1955]. With the absorbing gaseous mixture present, the observed quality factor of a cavity resonator, which is defined as the average stored electromagnetic energy divided by the energy dissipated per radian change in phase, is reduced due to the increase in losses. The measured quality factor of the gas-filled or "loaded" resonator can be written, per *Matthaei et al.* [1980], as

$$\frac{1}{Q_m} = \frac{1}{Q_c} + \frac{1}{Q_g} + \frac{1}{Q_{e1}} + \frac{1}{Q_{e2}}, \tag{2}$$

where Q_m is the measured quality factor of the gas-filled or loaded cavity resonator, Q_c is the quality factor of the evacuated cavity with no coupling losses, and Q_{e1}, Q_{e2} are the external quality factors due to coupling from the input and output ports of the cavity resonator, respectively.

In (2), Q_m is directly measured, since it can be expressed as $Q = f_r/\Delta f$, where f_r is the cavity resonant frequency and Δf is its half-power bandwidth. The term Q_c is controlled by losses due to imperfectly conducting walls in the cavity, as well as losses through apertures opened in the cavity resonator such as mode suppression slots. The term Q_g accounts for losses in the absorbing gaseous mixture, while Q_{e1} and Q_{e2} represent losses due to coupling from the input and output ports of the resonator, respectively. Assuming that the coupling ports are identical, then $Q_{e1} = Q_{e2} = Q_e$. Furthermore, note that Q_e is related to Q_m and the measured transmissivity (t_m) through a resonator at resonance, per *Matthaei et al.* [1980], by the following equation

$$Q_e = \frac{2Q_m}{\sqrt{t_m}}, \tag{3}$$

where t_m is given by

$$t_m = 10^{-S/10}, \tag{4}$$

and S (in dB) is the insertion loss of the cavity at its resonant frequency, which can be directly measured. Substituting (3) into (2) yields

$$\frac{1}{Q_m} = \frac{(1/Q_c) + (1/Q_g)}{1 - \sqrt{t_m}}. \tag{5}$$

Now, to find Q_g, one needs to subtract the measured quality factor of a gas-filled or loaded resonator (Q_{ml}) from the measured quality factor of a gas-empty or unloaded resonator (Q_{mu}), which gives [*DeBoer and Steffes*, 1994]

$$\frac{1}{Q_g} = \frac{1 - \sqrt{t_{ml}}}{Q_{ml}} - \frac{1 - \sqrt{t_{mu}}}{Q_{mu}}, \tag{6}$$

where t_{ml} is the measured transmissivity of the loaded (gas-filled) resonator and t_{mu} is the measured transmissivity of the unloaded (evacuated) resonator.

Consequently, the absorption coefficient for a relatively low loss gaseous mixture can be directly determined from the following expression:

$$\alpha \cong \frac{\pi}{\lambda}\left(\frac{1 - \sqrt{t_{ml}}}{Q_{ml}} - \frac{1 - \sqrt{t_{mu}}}{Q_{mu}}\right), \tag{7}$$

with λ in km and α in Nepers/km. Note that 1 Neper/km = 2 optical depths/km (or km^{-1})= 8.686 dB/km, where the third notation is used in this paper to avoid any ambiguities.

It should be noted that the above expression for the absorption coefficient assumes that the cavity's contribution to the overall measured Q is not dependent on the refractive (i.e., nonabsorptive) properties of the gas. However, this is not usually the case because the real part of the dielectric constant of the lossy gaseous mixture will alter the dielectric properties of the resonator and cause coupling variations from the input and output ports of the resonator; an effect commonly referred to as "dielectric loading" [see *Spilker*, 1993]. To remove the effects of dielectric loading, a lossless (nonabsorbing) gas should be used to measure the unloaded terms Q_{mu} and t_{mu}, such that the shifts in the resonant frequency for the lossy and lossless gases relative to vacuum are equal (i.e., identical refractive indices). Note that when a lossless gas is used, the above expression for the absorption coefficient is still valid, since $1/Q_g = 0$ for the nonabsorbing gas as well as for vacuum.

2.2. Experimental Apparatus

The experimental setup used to measure the temperature dependence of the microwave absorptivity of

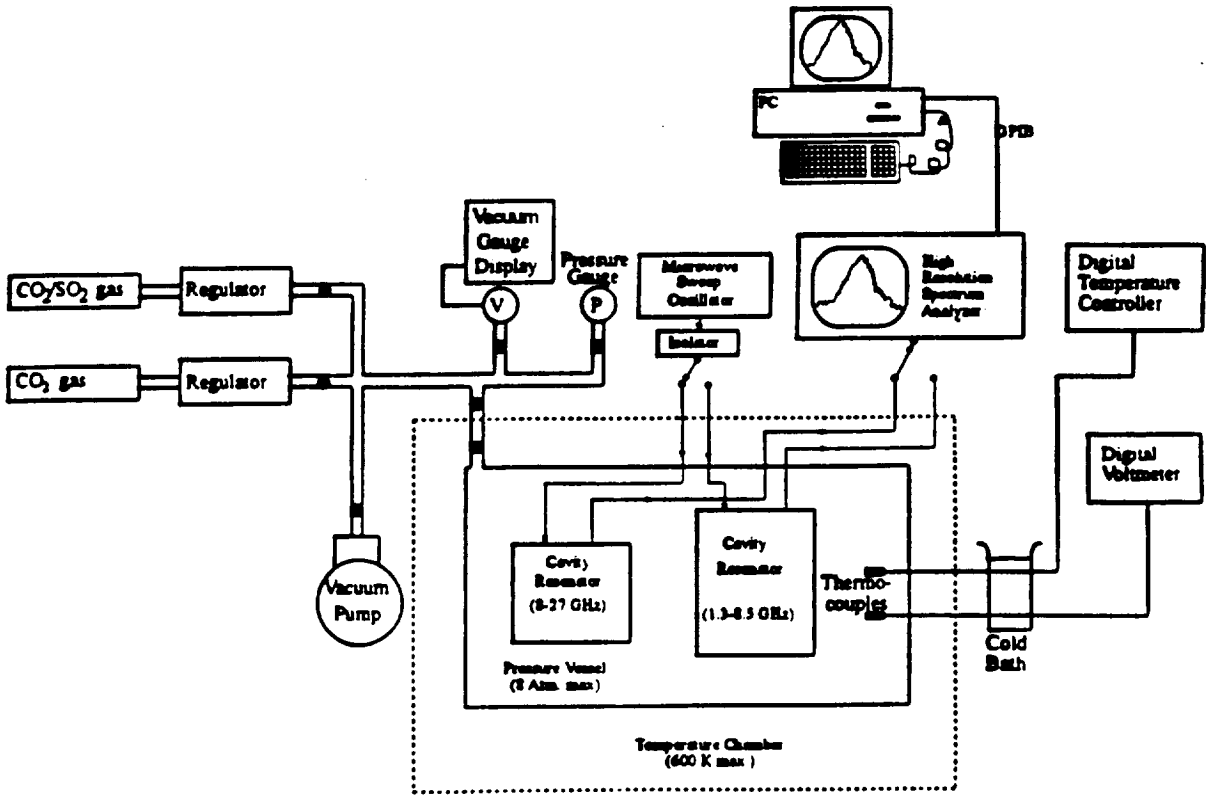

Figure 1. Block diagram of the experimental setup used to measure the temperature dependence of the microwave absorption of gaseous SO_2 under simulated conditions for the Venus atmosphere.

gaseous SO_2 in a CO_2 atmosphere under simulated Venus conditions is similar to that previously used by *DeBoer and Steffes* [1994] (also, D. R. DeBoer and P. G. Steffes, The Georgia Tech high sensitivity microwave measurement system, submitted to *Astrophysics and Space Science*, 1995) with minor modifications. Figure 1 illustrates the measurement system, which consists of a microwave subsystem, a Venus atmospheric simulator subsystem, and a data acquisition subsystem.

The microwave subsystem consists of two circular cylindrical cavity resonators. One cavity resonator is designed to operate in the frequency range 1.3-8.5 GHz and the other in the range 8-27 GHz. Each cavity has input and output ports with adjustable couplers used to couple energy into and out of the resonators. In addition, each cavity resonator incorporates two gaps to suppress the degenerate TM_{lmn} modes which have low-quality factors (Q's). The input port of each cavity resonator is connected to a microwave sweep oscillator. The oscillator consists of a main frame with a replaceable backward wave oscillator (BWO) module. For the purposes of this experiment, three BWO modules are used: the first module operates in the 2-4 GHz range (S band), the second module operates in the 8-12 GHz range (X band), while the third module operates in the 18-26 GHz range (K band). The output terminals of the S and X band BWO modules are fed to S and X band isolators, respectively, while the output terminal of the K band BWO module is fed to a 10-dB attenuator. Note that the attenuator and the isolators are used to minimise any reflected signal from the cavity resonator to the sweep oscillator. Moreover, the isolators permit essentially unattenuated transmission from the sweep oscillator to the cavity resonators. The output of each of the S and X band isolators is connected to the input port of the 1.3-8.5 GHz resonator via a flexible coaxial cable, whereas the output of the attenuator is connected to the input port of the 8-27 GHz resonator via a three-spline rigid coaxial cable. A high-resolution spectrum analyser (HP 8562B) is then used to measure the signal from the output ports of the two resonators.

The Venus atmospheric simulator subsystem consists of a stainless steel pressure vessel which contains the two cavity resonators. This containment vessel, which can withstand pressures up to 8 atm, is placed inside a digitally controlled temperature chamber that is capable of reaching temperatures up to 600 K. Two thermocouples which are suspended within the pressure vessel are used to monitor the temperature of the introduced gas. One thermocouple is connected to a digital voltmeter, while the other is connected to a digital temperature controller. Both the CO_2 gas cylinder and the SO_2/CO_2 gaseous mixture cylinder are connected to the pressure vessel via a network of 3/8-inch stainless-steel tubing. In addition, regulators and valves are included in the tubing network so that parts of the measurement system may be isolated to detect gas leaks and to ensure

safety. A vacuum pump that is capable of achieving 3 torr or less is used to evacuate the pressure vessel before admitting the gas. The vacuum status is monitored via a digital thermocouple vacuum gauge, which can measure pressures in the range 1 to 800 torr. For higher pressure measurements, an analog positive pressure gauge which is able to measure pressures in the range 0 to 7.8 atm is used, with ±0.2 atm accuracy throughout its usable range.

The final subsystem is responsible for data acquisition. This subsystem consists of a personal computer loaded with a software package that is used to interface with the HP 8562B spectrum analyser via a general purpose interface bus (GPIB) (D. R. DeBoer and P. G. Steffes, submitted manuscript, 1995). The software package reads, processes, and fits the spectrum data points. Then the resonant frequency, half-power bandwidth, and amplitude at the resonant frequency are found. If the spectrum measurement is repeated several times, then averages and variances are also computed by the software.

2.3. Experimental Procedure

The first step in the measurement process is to heat the entire system for sufficient time (approximately 12 hours) that thermal equilibrium is achieved at the desired experimental temperature. Then the pressure vessel is evacuated, and the cavity resonant frequency, the half-power bandwidth, and the amplitude at the resonant frequency are measured for three different resonances: 2.25 GHs (13.3 cm), 8.5 GHs (3.5 cm), and 21.7 GHs (1.4 cm). A premixed analysed SO_2/CO_2 gaseous mixture is then introduced slowly into the pressure vessel until the required pressure is reached. As the SO_2/CO_2 gaseous mixture is admitted, changes in the resonant frequency are observed. Thus, careful tracking of the desired resonance is important, since other resonances are present. Once the resonant frequency stabilises, the same measurements performed for the evacuated resonator are repeated for the gas-filled or loaded resonator and, consequently, Q_{ml} is determined. The pressure is then reduced by venting, and subsequent measurements are likewise conducted at lower pressures in order to determine the absorption coefficient of the SO_2/CO_2 gaseous mixture at those pressures. After completing the required measurements with the SO_2/CO_2 gaseous mixture, a vacuum is drawn in the pressure vessel, and the quality factor of each of the evacuated resonators is again measured to ensure its consistency. Next, gaseous CO_2 is introduced into the pressure vessel such that the refractive indices of the SO_2/CO_2 gaseous mixture and gaseous CO_2 are identical. The measurement procedure is then repeated, and Q_{mu} is determined. Note that by measuring Q_{mu} with gaseous CO_2 rather than with a vacuum, the effects of dielectric loading are removed. Also note that the small absorptivity due to the pure CO_2 gas is well below the detection sensitivity of the measurement system; thus it serves as a "lossless" reference [see *Ho et al.*, 1966]. The last step in the experimental procedure is to measure the amplitude of the transmitted signal directly from the microwave sweep oscillator to the spectrum analyser, which in turn, is used to determine the insertion loss of each cavity resonator at its resonant frequency. Consequently, t_{ml} and t_{mu} are determined.

3. Uncertainty Analysis

Laboratory measurements of the microwave opacity from gaseous SO_2 in a CO_2 atmosphere are subject to two classes of uncertainties. The first class is due to instrumental errors which are caused by the limited accuracy of the equipment used to measure the resonant frequency, half-power bandwidth, transmissivity, mixing ratio of the gaseous mixture, pressure, temperature, and resonance asymmetry. Table 1 shows the standard deviations of the resonant frequency (σ_{f_r}) and the half-power bandwidth measurements ($\sigma_{\Delta f}$) due to the spectrum analyser accuracy at 2.25 GHs, 8.5 GHs, and 21.7 GHs [*Hewlett-Packard Corporation*, 1986]. Uncertainties in the transmissivity measurement have been neglected, since the worst case variations in the expression $1-\sqrt{t}$ are less than 1%. In the case of the uncertainty in the mixing ratio of the gaseous mixture, a custom premixed, constituent-analysed SO_2/CO_2 gaseous mixture from Matheson Gas Company is used with ±2% uncertainty in the stated component mixing ratio. For pressure measurement, the analog pressure gauge has a ±0.2 atm uncertainty. In the case of temperature measurement, the digital temperature controller has ±0.25% of the input temperature span, which corresponds to ±2 K. Another effect known as "resonance asymmetry" may produce errors, since coupling from other resonances may distort the measured bandwidth of the resonance being monitered. The asymmetry figure of merit $A_{\Delta f}$ defined as

$$A_{\Delta f} = \frac{(f_h - f_r) - (f_r - f_l)}{f_h - f_l} \times 100\%, \qquad (8)$$

where f_h is the higher frequency at half-power transmissivity and f_l is the lower frequency at half-power transmissivity is monitored and recorded throughout the experiments. Note that for a perfectly symmetric resonance, $A_{\Delta f} = 0\%$. However, the measured resonances are not perfectly symmmetric. With the SO_2/CO_2 gaseous mixture present in the cavity resonator, the absolute asymmetry is about 1-5% at 2.25 GHs, 11-18% at 8.5 GHs, and 6-12% at 21.7 GHs. Even with CO_2 gas present, the corresponding resonance asymmetries are approximately equal to the values obtained as with

Table 1. Spectrum Analyser Instrument Uncertainty at Resonant Frequencies

Resonant Frequency, GHs	σ_{f_r}, KHs	$\sigma_{\Delta f}$, KHs
2.25	25	0.240
8.5	95	0.800
21.7	372	4.820

the SO_2/CO_2 present in the cavity. This implies that the phenomenon of resonance asymmetry is not induced by the introduction of the lossy gaseous mixture to the cavity. Thus the resonance asymmetry is most likely due to the impedance mismatch at the probe-to-cable interface, which is a function of frequency. However, since the effects of dielectric loading in these experiments are removed (i.e., impedance mismatch effects are also removed), the impact of resonance asymmetry on absorptivity measurements is generally negligible.

The other important class of uncertainties results from the random electrical noise in the system. This noise is caused by the large insertion loss of the cavities (due to minimal coupling), which is necessary to maintain high-quality factors. The two quantities that are influenced by the electrical noise are the resonant frequency and the half-power bandwidth. For repeated measurements, where 20 data points are recorded per frequency, pressure, and temperature, it is found that the resonant frequency can be measured very accurately (variance $\leq 0.01\%$). However, the bandwidth measurements are significantly affected by the random noise, which in turn, influences the measured quality factor. Assuming Gaussian statistics, the total standard deviation in the 20 bandwidth measurements taken for each measured absorption coefficient is obtained by multiplying the sample standard deviation in the bandwidth with a scale factor called the confidence interval, which is normalized to the square root of the number of repeated measurements [e.g., *Kreyszig*, 1983]. For the 20 bandwidth measurements, a 3.55 confidence interval has been used, which corresponds to a 0.999 confidence level. Thus the variance of the repeated bandwidth measurements is included in the uncertainty of the measured absorption coefficient.

The total uncertainty in the measured absorption coefficient (α) is determined by incorporating the individual uncertainties into a "worst case" uncertainty expression which would give the overall one-sigma error [see *DeBoer and Steffes*, 1994]. Note that the worst case uncertainty expression accounts for the correlation between the errors in bandwidth and resonant frequency measurements for both the loaded and unloaded resonators.

4. Results and Interpretation

4.1 Experimental Results

High-accuracy laboratory measurements of the temperature dependence of the microwave absorption from gaseous SO_2 in a CO_2 atmosphere have been conducted at temperatures from 290 to 505 K and at pressures from 1 to 4 atm for the following frequencies (wavelengths): 2.25 GHz (13.3 cm), 8.5 GHz (3.5 cm), and 21.7 GHz (1.4 cm). Tables 2, 3, 4, and 5 show the results of these absorptivity measurements with the one-sigma uncertainty at 295, 365, 435, and 505 K, respectively. For comparison purposes, these tables also show the calculated absorptivity of the SO_2/CO_2 gaseous mixture using the developed BR line shape model, which is discussed below. In addition, the value of χ^2_{BR}, which is a measure of the goodness of the fitting function (of

Table 2. Measured Microwave Absorption of Gaseous SO_2 in a CO_2 Atmosphere at 295 K for Various Pressures and Frequencies

Date	Pressure, atm	Frequency, GHz	Mixing Ratio, %	Measured α, dB/km	Calculated α, dB/km	χ^2_{BR}
April 28, 1994	4.06	2.25	8.30	0.743 ± 0.037	0.688	2.236
	4.06	8.5	8.30	10.205 ± 0.138	9.717	12.493
	4.06	21.7	8.30	63.899 ± 2.207	61.916	0.808
	3.04	2.25	8.30	0.452 ± 0.038	0.490	1.040
	3.04	8.5	8.30	6.931 ± 0.162	6.875	0.122
	3.04	21.7	8.30	49.062 ± 2.870	43.575	3.655
	2.02	2.25	8.30	0.397 ± 0.038	0.307	5.567
	2.02	8.5	8.30	4.113 ± 0.154	4.252	0.819
	2.02	21.7	8.30	28.603 ± 2.447	26.990	0.434
May 16, 1994	4.06	2.25	8.30	0.613 ± 0.037	0.688	4.010
	4.06	8.5	8.30	10.004 ± 0.134	9.717	4.611
	4.06	21.7	8.30	60.981 ± 2.218	61.916	0.178
	3.38	2.25	8.30	0.541 ± 0.037	0.555	0.137
	3.38	8.5	8.30	7.849 ± 0.148	7.801	0.106
	3.38	21.7	8.30	52.941 ± 2.933	49.513	1.366
	2.36	2.25	8.30	0.282 ± 0.037	0.367	5.214
	2.36	8.5	8.30	4.860 ± 0.138	5.097	2.930
	2.36	21.7	8.30	36.528 ± 2.786	32.297	2.306
	1.68	2.25	8.30	0.142 ± 0.041	0.249	6.821
	1.68	8.5	8.30	3.476 ± 0.137	3.445	0.051
	1.68	21.7	8.30	21.389 ± 2.612	21.924	0.042
June 8, 1994	4.06	2.25	8.30	0.616 ± 0.037	0.688	3.745
	3.38	2.25	8.30	0.502 ± 0.036	0.555	2.134
	3.04	2.25	8.30	0.461 ± 0.036	0.490	0.640
	2.36	2.25	8.30	0.325 ± 0.037	0.367	1.244
	2.02	2.25	8.30	0.216 ± 0.038	0.307	5.658

Table 3. Measured Microwave Absorption of Gaseous SO_2 in a CO_2 Atmosphere at 365 K for Various Pressures and Frequencies

Date	Pressure, atm	Frequency, GHz	Mixing Ratio, %	Measured α, dB/km	Calculated α, dB/km	χ^2_{BR}
June 24, 1994	4.06	2.25	8.30	0.348 ± 0.046	0.381	0.524
	4.06	8.5	8.30	5.615 ± 0.235	5.36	1.191
	4.06	21.7	8.30	29.346 ± 3.157	33.93	2.104
	3.04	2.25	8.30	0.319 ± 0.048	0.274	0.936
	3.04	8.5	8.30	3.790 ± 0.187	3.816	0.019
	3.04	21.7	8.30	17.471 ± 2.974	24.091	4.956
	2.02	2.25	8.30	0.116 ± 0.059	0.173	0.922
	2.02	8.5	8.30	2.228 ± 0.164	2.389	0.955
	2.02	21.7	8.30	7.275 ± 2.920	15.137	7.249
Aug.1, 1994	4.06	2.25	8.97	0.342 ± 0.066	0.411	1.107
	4.06	8.5	8.97	5.674 ± 0.297	5.786	0.144
July 31, 1994	4.06	21.7	8.97	32.304 ± 3.060	36.672	2.037
Aug.1,1994	3.04	2.25	8.97	0.253 ± 0.078	0.296	0.299
	3.04	8.5	8.97	3.974 ± 0.230	4.121	0.415
July 31, 1994	3.04	21.7	8.97	23.896 ± 4.441	26.042	0.234
Aug.1, 1994	2.02	8.5	8.97	2.299 ± 0.207	2.580	1.847
July 31, 1994	2.02	21.7	8.97	13.747 ± 2.853	16.359	0.838

the developed BR formalism) with respect to the results of the absorptivity measurements, is also shown in the tables (note that a smaller value of χ^2_{BR} implies a better fit). For comparison purposes, Table 6 gives the χ^2 values obtained using the new BR formalism, the VVW model [*Van-Vleck and Weisskopf*, 1945], the Gross (GR) model [*Gross*, 1955], the Janssen and Poynter (JP) model [*Janssen and Poynter*, 1981], and the Steffes and Eshleman (SE) model [*Steffes and Eshleman*, 1981]. This table also gives the total of the χ^2 values for each formalism, which shows that the new BR formalism has the smallest χ^2 total. Thus the new BR model provides a better overall fit to the measured microwave absorption of gaseous SO_2 in a CO_2 atmosphere. Figures 2, 3, and 4 show the measured absorptivity (normalised to number mixing ratio) as a function of temperature at 4 atm for frequencies 2.25, 8.5, 21.7 GHz, respectively. Also shown in these figures are the calculated absorptivities using the developed BR, VVW, GR, JP, and SE models. Note from these figures that the developed BR formalism provides a more accurate characterisation of the microwave absorption of gaseous SO_2 in a CO_2 environment as compared to the other formalisms. Figure 5 presents the measured normalised absorptivity as a function of temperature at 2 atm for a frequency of 8.5 GHz. From this figure, it is clear that the developed BR model fits well the measured data even at low pressures. Other models are also shown in the figure for comparison. Figures 6 and 7 show the measured absorptivity (normalised to number mixing ratio) as a function of frequency at 4 atm for 295 K and 505 K, repectively. Again, one can see that the developed BR formalism results in a better fit to the measured data as compared to other models for both

Table 4. Measured Microwave Absorption of Gaseous SO_2 in a CO_2 Atmosphere at 435 K for Various Pressures and Frequencies

Date	Pressure, atm	Frequency, GHz	Mixing Ratio, %	Measured α, dB/km	Calculated α, dB/km	χ^2_{BR}
Aug.4, 1994	4.06	2.25	8.97	0.223 ± 0.078	0.254	0.153
	4.06	8.5	8.97	2.808 ± 0.231	3.555	10.477
Aug.21, 1994	4.06	21.7	8.97	27.989 ± 5.528	22.455	1.002
Aug.4, 1994	3.04	2.25	8.97	0.140 ± 0.062	0.184	0.494
	3.04	8.5	8.97	2.226 ± 0.230	2.546	1.929
Aug.21, 1994	3.04	21.7	8.97	18.780 ± 5.853	16.071	0.217
	2.02	2.25	8.97	0.053 ± 0.079	0.116	0.637
Aug.4, 1994	2.02	8.5	8.97	1.490 ± 0.236	1.612	0.267
Aug.21, 1994	2.02	21.7	8.97	11.347 ± 6.723	10.216	0.028
	4.06	2.25	8.97	0.289 ± 0.065	0.254	0.290
	4.06	8.5	8.97	3.277 ± 0.155	3.555	3.228
Sept.22, 1994	4.06	21.7	8.97	33.246 ± 6.224	22.455	3.006
Aug.21, 1994	3.04	2.25	8.97	0.249 ± 0.089	0.184	0.548
	3.04	8.5	8.97	2.531 ± 0.182	2.546	0.007
Sept.22, 1994	3.04	21.7	8.97	20.580 ± 6.252	16.071	0.520
Aug.21, 1994	2.02	8.5	8.97	1.162 ± 0.144	1.612	9.782
Sept.22, 1994	2.02	21.7	8.97	15.301 ± 4.948	10.216	1.015

Table 5. Measured Microwave Absorption of Gaseous SO_2 in a CO_2 Atmosphere at 505 K for Various Pressures and Frequencies

Date	Pressure, atm	Frequency, GHz	Mixing Ratio, %	Measured α, dB/km	Calculated α, dB/km	χ^2_{BR}
Oct.25, 1994	4.06	2.25	8.66	0.252 ± 0.145	0.163	0.377
	4.06	8.5	8.66	2.436 ± 0.173	2.274	0.883
Dec.31, 1994	4.06	21.7	8.66	11.905 ± 3.428	14.336	0.503
Oct.25, 1994	3.04	2.25	8.66	0.075 ± 0.091	0.118	0.223
	3.04	8.5	8.66	1.578 ± 0.163	1.636	0.126
Sept.23, 1994	3.04	21.7	8.97	13.230 ± 7.703	10.700	0.108
Oct.25, 1994	2.02	2.25	8.66	0.058 ± 0.099	0.075	0.030
	2.02	8.5	8.66	1.153 ± 0.150	1.046	0.513
Sept.23, 1994	2.02	21.7	8.97	7.731 ± 7.995	6.869	0.012
Oct.26, 1994	4.06	2.25	8.66	0.188 ± 0.100	0.163	0.062
	4.06	8.5	8.66	2.488 ± 0.170	2.274	1.593
Jan.1, 1995	4.06	21.7	8.66	11.496 ± 2.520	14.336	1.270
Oct.26, 1994	3.04	8.5	8.66	1.685 ± 0.173	1.636	0.082
Sept.24, 1994	3.04	21.7	8.97	11.095 ± 6.962	10.70	0.003
Oct.26, 1994	2.02	2.25	8.66	0.046 ± 0.070	0.075	0.169
	2.02	8.5	8.66	1.036 ± 0.160	1.046	0.004
Sept.24, 1994	2.02	21.7	8.97	5.856 ± 6.532	6.869	0.024

the highest and lowest temperatures. However, it can be noticed from Figure 3 that one pair of measured absorptivities is inconsistent (error bars do not overlap). This inconsistency at 435 K is likely due to errors in the temperature measurement, which might have been caused by improper closure of the valve inside the temperature chamber.

Overall, this new BR formalism provides a substantial improvement over previous models when compared to our absorptivity measurements.

4.2. Absorptivity Modeling Results

Based on the measurements of the temperature dependence of the microwave absorption from gaseous SO_2 in a CO_2 atmosphere, a new BR line shape model that provides a more accurate characterisation of gaseous SO_2 absorptivity in the Venus atmosphere has been developed. In general, the absorption model can be written for a single SO_2 rotational resonant line as

$$\alpha = \alpha_{max}\pi\gamma f_{shape}(\nu, \nu_o, \ldots) \quad \text{cm}^{-1}, \quad (9)$$

where α_{max} is the absorption at the line center in cm^{-1}, γ is the linewidth in MHs, f_{shape} is the spectral line shape function in MHs^{-1}, ν is the frequency of interest in MHs, and ν_o is the line center frequency in MHs.

Now, the absorption at the line center α_{max} for each line of gaseous SO_2 is calculated using the following expression [*Poynter and Pickett*, 1985]

$$\alpha_{max} = 102.46\frac{P_{SO_2}}{\gamma} I(T_o)\left(\frac{T_o}{T}\right)^{7/2} e^{-(hc/k)E_l(1/T-1/T_o)} \quad \text{cm}^{-1}, \quad (10)$$

where P_{SO_2} is the partial pressure of gaseous SO_2 in torr, I is the line center intensity in nm^2MHs, T_o is the reference temperature (T_o = 300 K), E_l is the lower state energy in cm^{-1}, k is Boltzmann's constant = 1.38×10^{-23} J/K, h is Planck's constant = 6.63×10^{-34} J.s, and c is the speed of light in free space = 3×10^{10} cm/s.

Note that the total absorption coefficient at a particular frequency is obtained by summing over all of the individual SO_2 line center intensities up to 750 GHs (1587 resonant lines) which are obtained from the *Poynter and Pickett* [1985] catalog.

For the spectral line shape function f_{shape}, a BR line shape expression [*Ben-Reuven*, 1966] has been used in modeling the microwave absorption from gaseous SO_2 in a CO_2 atmosphere. This expression takes into account the effect of overlapping and merging of distinct resonance lines and is applicable to centimeter wavelength absorption even at pressures where the linewidth is comparable to the resonant frequency. The spectral line shape according to Ben-Reuven is written as

$$f_{BR}(\nu, \nu_o, \gamma, \varsigma, \delta) = \frac{2}{\pi}\left(\frac{\nu}{\nu_o}\right)^2 \cdot \frac{(\gamma-\varsigma)\nu^2 + (\gamma+\varsigma)[(\nu_o+\delta)^2+\gamma^2-\varsigma^2]}{[\nu^2-(\nu_o+\delta)^2-\gamma^2+\varsigma^2]^2+4\nu^2\gamma^2} \quad \text{MHz}^{-1}, \quad (11)$$

where the linewidth γ, the coupling element ς, and the frequency shift element δ can be expressed as

$$\gamma = (\gamma_{SO_2/CO_2})P_{CO_2}\left(\frac{T_o}{T}\right)^n + (\gamma_{SO_2/SO_2})P_{SO_2}\left(\frac{T_o}{T}\right)^n \quad \text{MHs}, \quad (12)$$

$$\varsigma = (\varsigma_{SO_2/CO_2})P_{CO_2}\left(\frac{T_o}{T}\right)^m + (\varsigma_{SO_2/SO_2})P_{SO_2}\left(\frac{T_o}{T}\right)^m \quad \text{MHs}, \quad (13)$$

Table 6. Goodness of Fit Function (χ^2) using the New Ben-Reuven (BR), Van-Vleck and Weisskopf (VVW), Janssen and Poynter (JP), Gross (GR), and Steffes and Eshleman (SE) Formalisms

χ^2_{BR}	χ^2_{VVW}	χ^2_{JP}	χ^2_{GR}	χ^2_{SE}
2.236	16.262	4.396	1018.951	190.260
12.493	152.883	118.805	1936.638	3099.089
0.808	11.333	31.652	75.861	570.018
1.040	0.538	10.801	465.214	130.502
0.122	28.407	63.945	450.253	1242.184
3.655	8.853	2.522	4.528	134.869
5.567	11.807	1.506	70.257	14.677
0.819	3.349	32.949	92.965	555.227
0.434	1.358	2.621	2.161	79.707
4.010	0.286	31.297	1254.489	298.987
4.611	126.333	161.696	2190.938	3459.356
0.178	4.137	47.780	99.644	628.602
0.137	2.794	9.688	641.444	157.876
0.106	44.773	104.648	873.645	1933.678
1.366	6.070	7.593	14.075	191.886
5.214	0.903	14.555	269.561	100.800
2.930	5.016	73.115	250.909	1048.206
2.306	4.628	1.040	0.983	75.922
6.821	3.293	11.274	100.252	51.006
0.051	5.969	14.085	36.348	396.511
0.042	0.011	3.125	2.686	53.189
3.745	0.363	30.549	1249.73	296.666
2.134	0.406	18.312	734.826	195.802
0.640	1.104	10.187	505.578	138.744
1.244	0.047	7.007	232.567	78.708
5.658	1.695	12.327	172.133	73.429
0.524	0.145	2.751	213.917	42.579
1.191	14.303	3.454	139.538	238.710
2.104	0.425	10.226	20.265	95.865
0.936	2.963	0.219	55.632	8.204
0.019	4.229	6.105	73.237	215.264
4.956	3.127	11.857	16.125	71.294
0.922	0.342	1.197	20.349	7.718
0.955	0.076	4.651	20.598	116.726
7.249	6.312	10.707	12.511	41.444
1.107	0.056	3.114	134.051	29.463
0.144	3.557	8.514	133.470	211.391
2.037	0.297	11.376	23.737	115.007
0.299	0.003	0.782	38.177	9.600
0.415	1.584	7.320	66.417	180.273
0.234	0.024	1.858	3.218	24.817
1.847	0.088	5.641	19.887	95.618
0.838	0.516	2.423	3.457	25.584
0.153	0.001	0.299	30.912	5.502
10.477	2.446	18.328	116.546	167.841
1.002	1.572	0.345	0.000	3.151
0.494	0.110	0.574	23.114	5.645
1.929	0.101	3.677	27.655	66.275
0.217	0.349	0.058	0.004	1.828
0.637	0.386	0.581	5.996	2.406
0.267	0.000	0.304	3.515	18.671
0.028	0.043	0.014	0.003	0.556
0.290	1.072	0.123	32.092	3.268
3.228	0.485	11.242	170.580	265.004
3.006	3.835	1.866	0.716	0.536
0.548	0.998	0.493	4.490	0.181
0.007	1.612	0.566	24.747	74.248
0.520	0.702	0.261	0.052	0.962
9.782	5.283	10.136	28.660	87.678
1.015	1.127	0.880	0.504	0.055
0.377	0.569	0.388	1.144	0.001
0.883	5.203	0.549	21.549	39.672
0.503	0.238	0.837	2.578	10.438
0.223	0.098	0.178	4.641	1.191
0.126	0.286	0.072	11.050	31.435
0.108	0.144	0.088	0.009	0.217
0.030	0.007	0.013	0.914	0.246
0.513	1.366	1.265	0.168	6.156
0.012	0.016	0.018	0.000	0.103
0.062	0.205	0.069	4.800	0.350
1.593	6.902	1.123	19.529	37.274
1.270	0.681	1.980	5.506	20.767
0.082	1.265	0.136	6.303	21.721
0.003	0.013	0.001	0.041	0.676
0.169	0.082	0.105	2.302	0.749
0.004	0.129	0.101	1.255	9.372
0.024	0.018	0.015	0.085	0.463
		Total		
133.726	518.009	976.355	14292.682	17610.096

$$\delta = \delta_{SO_2} P_{SO_2} \quad \text{MHs}, \tag{14}$$

where γ_{SO_2/CO_2} is the foreign gas broadened linewidth parameter in MHs/torr, γ_{SO_2/SO_2} is the self-broadened linewidth parameter in MHs/torr, ζ_{SO_2/CO_2} is the foreign gas coupling parameter in MHs/torr, ζ_{SO_2/SO_2} is the self-coupling parameter in MHs/torr, δ_{SO_2} is the frequency shift parameter in MHs/torr, P_{CO_2} is the partial pressure of gaseous CO_2 in torr, n is the temperature dependence of the linewidth, and m is the temperature dependence of the coupling element.

From the above discussion, it is evident that seven parameters for the BR spectral line shape function are needed in order to fit the absorptivity measurements. These parameters are γ_{SO_2/CO_2}, γ_{SO_2/SO_2}, ζ_{SO_2/CO_2}, ζ_{SO_2/SO_2}, δ_{SO_2}, n, and m. However, γ_{SO_2/CO_2} was measured in the laboratory for one resonant line at 24.08 GHs, and for that line it is 7.2 MHs/torr [*Krishnaji and Chandra*, 1963]. Furthermore, *Kolbe et al.* [1976] use a self-broadened linewidth parameter γ_{SO_2/SO_2} of 16 MHs/torr as an average value of the measured linewidth parameters which range from 13 to 19 MHs/torr. These values of 7.2 MHs/torr and 16 MHs/torr for γ_{SO_2/CO_2} and γ_{SO_2/SO_2}, respectively, are thus assumed for all SO_2 resonant lines, although it is likely that γ_{SO_2/CO_2} and γ_{SO_2/SO_2} vary from line to line. To determine the rest of the parameters, the goodness of fit function χ^2 [e.g., *Bevington*, 1969] has been globally minimized to fit all of the absorptivity measurements. Note that the goodness of fit function χ^2 can be written as

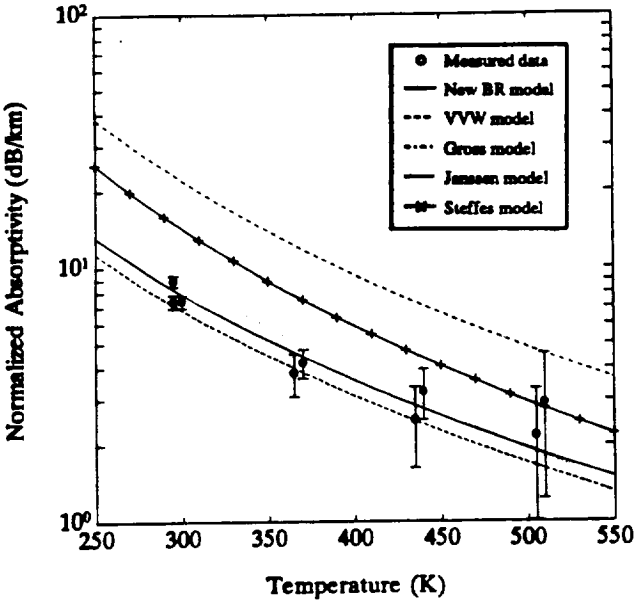

Figure 2. Measured absorptivity (normalised by number mixing ratio) of gaseous SO_2 in a CO_2 atmosphere as a function of temperature at 4 atm for a frequency of 2.25 GHs. The abscissa of the data points has been shifted from the actual temperature value for clarity. The 1-σ error in the temperature measurement is ± 2 K.

$$\chi^2 = \sum_{i=1}^{k} \frac{1}{\sigma_i^2} [\alpha_{m_i} - \alpha_{c_i}]^2, \qquad (15)$$

where α_{m_i} is the measured absorption coefficient, α_{c_i} is the calculated absorption coefficient, σ_i is the uncertainty in the measured absorption coefficient, and k is the number of measured absorption coefficients.

Now, global minimisation is achieved by introducing a set of values for the parameters ζ_{SO_2/CO_2}, ζ_{SO_2/SO_2}, δ_{SO_2}, n, and m and computing the goodness of fit func-

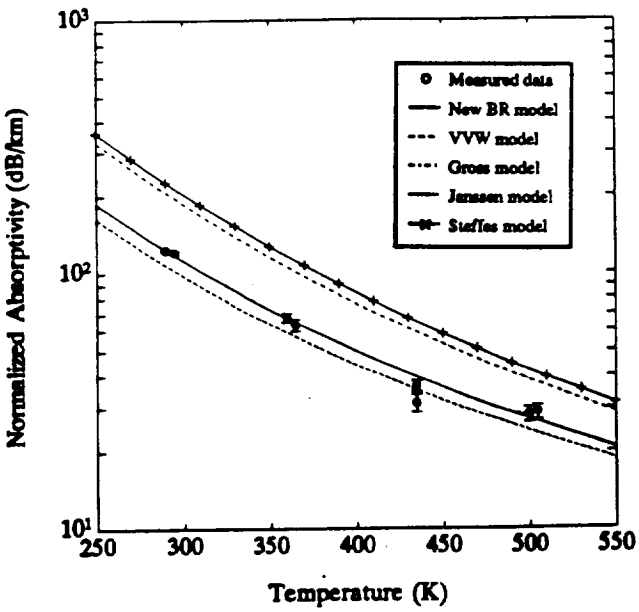

Figure 3. Measured absorptivity (normalised by number mixing ratio) of gaseous SO_2 in a CO_2 atmosphere as a function of temperature at 4 atm for a frequency of 8.5 GHs. The abscissa of the data points has been shifted from the actual temperature value for clarity. The 1-σ error in the temperature measurement is ± 2 K.

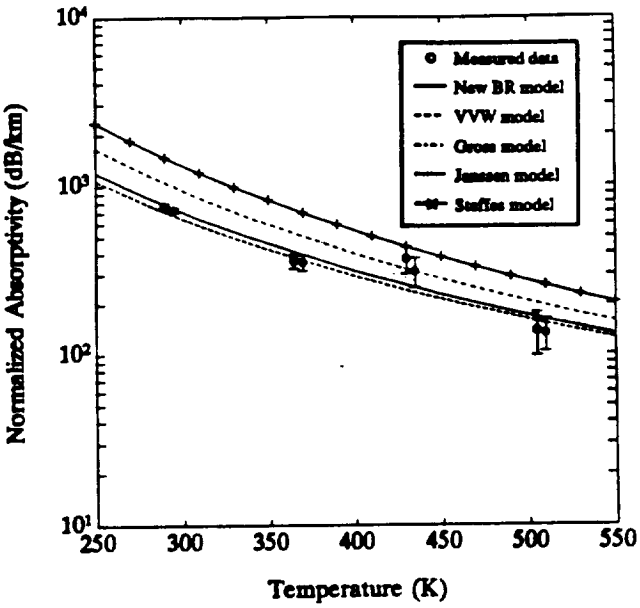

Figure 4. Measured absorptivity (normalised by number mixing ratio) of gaseous SO_2 in a CO_2 atmosphere as a function of temperature at 4 atm for a frequency of 21.7 GHs. The abscissa of the data points has been shifted from the actual temperature value for clarity. The 1-σ error in the temperature measurement is ± 2 K.

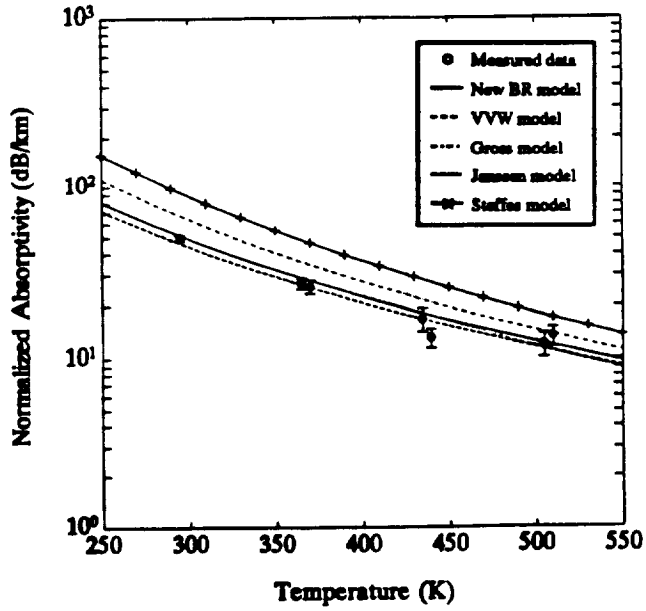

Figure 5. Measured absorptivity (normalised by number mixing ratio) of gaseous SO_2 in a CO_2 atmosphere as a function of temperature at 2 atm for a frequency of 8.5 GHs. The abscissa of the data points has been shifted from the actual temperature value for clarity. The 1-σ error in the temperature measurement is ± 2 K.

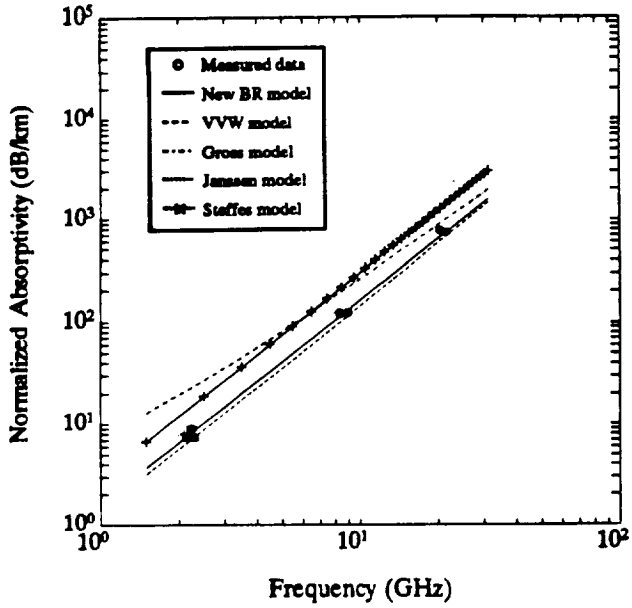

Figure 6. Measured absorptivity (normalised by number mixing ratio) of gaseous SO_2 in a CO_2 atmosphere as a function of frequency at 4 atm for 295 K. The abscissa of the data points has been shifted from the actual frequency value for clarity.

tion χ^2 for all absorptivity measurements until χ^2 converges to a minimum. Note that at the beginning of the search for the combination of optimal values for the above parameters, all values were varied including those for n and m. However, during the initial search it was found that varying n and m between 0.5 and 1 had a slight impact on the quality of fit. Therefore we let n equal m and continued the search until the goodness of fit function χ^2 was minimised. However, it is important to emphasise that the absorptivity calculated by the developed BR formalism is nearly insensitive to the parameters n and m. For example, setting n and m to 0.5, which is the lower limit of the temperature dependence of the linewidth, results in only about 3.2% change in the absorption coefficient at 2.25, 8.5, and 21.7 GHs for the highest pressure of 4 atm, and the highest temperature of 505 K. Even for the upper limit of 1, the absorption coefficient changes by only about 1.3%. Hence n and m are not key parameters in the fitting procedure. This procedure has been repeated for more than 75 sets of values, until convergence. Table 7 shows the values of parameters for the developed BR formalism that would yield the best fit for all microwave absorptivity measurements of the gaseous SO_2/CO_2 mixture.

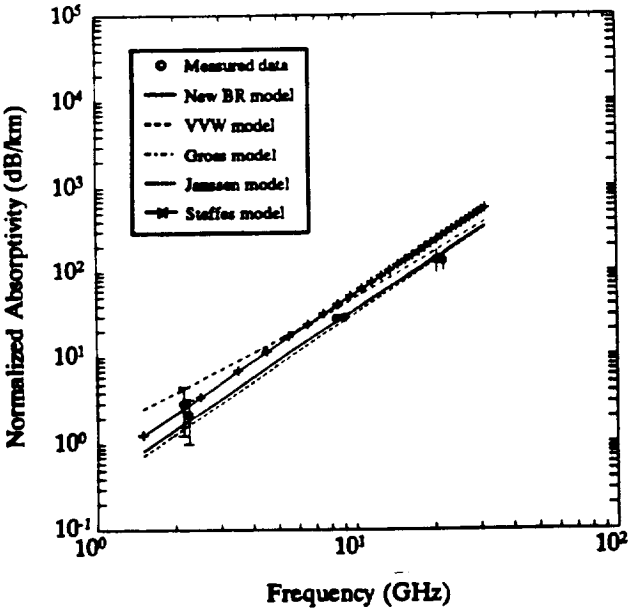

Figure 7. Measured absorptivity (normalised by number mixing ratio) of gaseous SO_2 in a CO_2 atmosphere as a function of frequency at 4 atm for 505 K. The abscissa of the data points has been shifted from the actual frequency value for clarity.

Table 7. Values of Parameters Used in the Developed Ben-Reuven Formalism

Parameter	Value
γ_{SO_2/CO_2}	7.2 MHs/torr
γ_{SO_2/SO_2}	16 MHs/torr
ζ_{SO_2/CO_2}	1.3 MHs/torr
ζ_{SO_2/SO_2}	1.6 MHs/torr
δ_{SO_2}	2.9 MHs/torr
$n = m$	0.85

5. Application

The developed formalism for the opacity of gaseous SO_2 under simulated Venus conditions has been incorporated into a radiative transfer model to compute disk-averaged brightness temperatures of Venus in the microwave region of its emission spectrum. In the model the pressure-temperature profile obtained from the Pioneer-Venus Sounder Probe is employed, and a physical surface temperature of 733 K is used [Seiff et al., 1980]. A mean surface dielectric permittivity of 4.5 is assumed [*Pettengill et al.*, 1992], yielding a disk-averaged surface emissivity of 0.841. The expression from *Ho et al.* [1966] for the opacity of gaseous CO_2 and gaseous N_2 in the Venus atmosphere is used, assuming a CO_2 and N_2 mixing ratio of 96.5% and 3.5%, respectively. Below the 48-km cloud layer, it is assumed that gaseous SO_2 molecules are uniformly mixed within the atmosphere and that above the cloud layer, the SO_2 abundance falls off exponentially with a scale height of 3.3 km [*Na et al.*, 1994].

The disk-averaged brightness temperatures are plotted in Figures 8 and 9 as a function of frequency for gaseous SO_2 mixing ratios below the main cloud layer of 0, 75, and 150 ppm. Also plotted in Figure 9 are microwave observations of the disk-averaged brightness temperature of Venus from *Steffes et al.* [1990]. There is good agreement between our model and the observed brightness temperatures except for the *X* band (8.42 GHs) observation. The discrepancy at *X* band is also observed using the radiative transfer model of *Muhleman et al.* [1979].

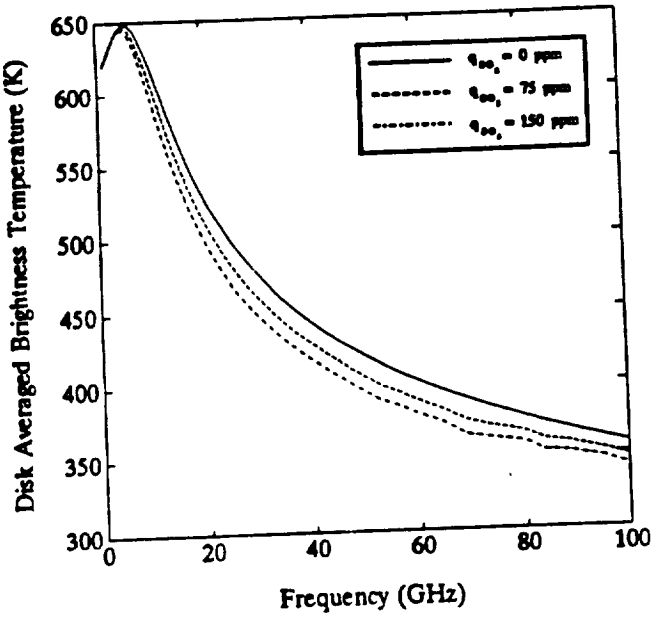

Figure 8. Plot of the disk-averaged brightness temperatures of Venus as a function of frequency for gaseous SO_2 mixing ratios below the main cloud layer of 0, 75, and 150 ppm.

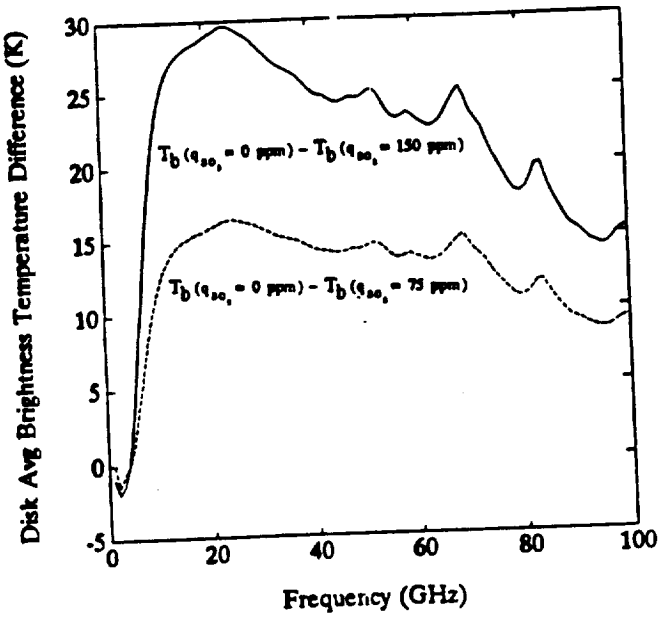

Figure 10. Plots of the difference in disk-averaged brightness temperature between a Venus atmosphere with only CO_2-N_2 and a Venus atmosphere with CO_2-N_2 and SO_2.

It is useful to plot the difference in the disk-averaged brightness temperature between a Venus atmosphere with only CO_2-N_2 and a Venus atmosphere with CO_2-N_2 and SO_2. Such a plot is shown in Figure 10. The largest drop in the brightness temperature due to SO_2 opacity occurs in the *K* band portion of the emission spectrum between 20 and 25 GHs. Observations in this region would be most sensitive to detecting gaseous SO_2. Table 8 lists our modeling results for an emission frequency of 22.2 GHs.

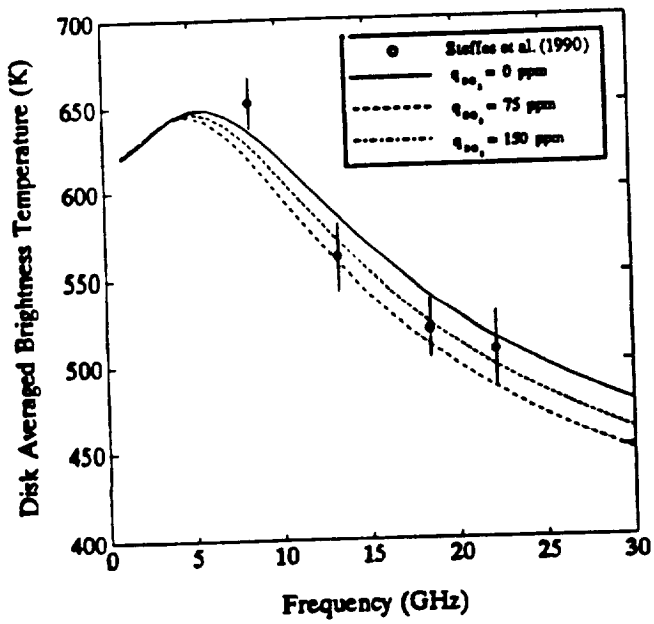

Figure 9. An expansion of Figure 8, showing the centimeter-wave disk-averaged brightness temperatures of Venus. Also plotted are Venus microwave observations from *Steffes et al.* [1990].

The *K* band atmospheric weighting functions peak between 25 and 35 km above the Venus surface. The measured disk-averaged brightness temperature at 22.2 GHs from *Steffes et al.* [1990] is 507 ± 22 K. The resulting upper limit on the mixing ratio of gaseous SO_2 below the main cloud layer (based on uniform mixing) is 150 ppm, which corresponds to the -1 σ error bar of the measured *K* band emission. Our result is in agreement with recent infrared Earth-based observations [see *Besard et al.*, 1993]. This upper limit also compares well with previous spacecraft in situ measurements [see *Oyama et al.*, 1980; *Gelman et al.*, 1979]. Further details of this radiative transfer model will be described in a future paper by Kolodner and Steffes.

The abundance of gaseous SO_2 can be more tightly constrained once the absorptivity properties of another important microwave absorber below the main cloud layer, sulfuric acid vapor, are well understood. Laboratory measurements are currently under way to measure more accurately the opacity of gaseous H_2SO_4 in a CO_2 environment. There are also plans to perform observations of Venus at 1.3 cm and 2 cm with the very large array to obtain high-resolution emission maps of Venus. These maps could be used to infer large-scale spatial variations in the abundances of gaseous SO_2 and gaseous H_2SO_4 across the disk of the planet.

6. Conclusions and Future Work

High-accuracy laboratory measurements of the temperature dependence of the microwave absorption from gaseous SO_2 in a CO_2 atmosphere have been conducted at temperatures from 290 to 505 K and at

Table 8. Results From Out Venus Microwave Radiative Transfer Model at an Emission Frequency of 22.2 GHz

SO_2 Mixing Ratio Below 48 km, ppm	Optical Depth of Venus, Optical Depths	Disk-Averaged Surface Weighting Function	Disk-Averaged Brightness Temperature, K
0	5.87	6.62×10^{-4}	514.20
75	6.63	2.82×10^{-4}	498.03
150	7.40	1.21×10^{-4}	484.84

pressures from 1 to 4 atm for the following frequencies (wavelengths): 2.25 GHs (13.3 cm), 8.5 GHs (3.5 cm), and 21.7 GHs (1.4 cm). Based on these measurements, a new BR line shape model has been developed. This model provides more accurate characterisation of gaseous SO_2 absorptivity in the Venus atmosphere as compared to other formalisms. In addition, the new BR formalism is incorporated into a radiative transfer model to explain the microwave emission spectrum of Venus and to infer more accurate abundance estimates of gaseous SO_2 in the Venus atmosphere. This new formalism for the opacity of gaseous SO_2 in a CO_2 environment can be used to infer limits on the abundances of gaseous SO_2 from the 3.6-cm absorptivity profiles of the Venus atmosphere obtained from the Magellan radio occulation experiments [*Jenkins et al.*, 1994]. It will also be used in a radiative transfer model especially for 1.3-cm emission maps of Venus to infer new abundance estimates of gaseous SO_2 in the Venus atmosphere.

Acknowledgments. The authors thank graduate student David DeBoer of the Georgia Institute of Technology for providing the data acquisition software and for his valuable suggestions during the experiments. We also thank the reviewers for their constructive comments, which improved the quality of this paper. This work was supported by the Planetary Atmospheres Program of the National Aeronautics and Space Administration under grant NAGW-533.

References

Ben-Reuven, A., Impact broadening of microwave spectra, *Phys. Rev., 145*, 7-22, 1966

Bevington, P. R., *Data Reduction and Error Analysis for the Physical Sciences*, pp. 187-203, 1969.

Besard, B., C. de Bergh, B. Fegley, J.P. Maillard, D. Crisp, T. Owen, J. B. Pollack, and D. Grinspoon, The abundance of sulfur dioxide below the clouds of Venus, *Geophy. Res. Lett., 20*, 1587-1590, 1993.

DeBoer, D. R., and P. G. Steffes, Laboratory measurements of the microwave properties of H_2S under simulated Jovian conditions with an application to Neptune, *Icarus, 109*, 352-366, 1994.

Fahd, A. K., and P. G. Steffes, Laboratory measurements of the microwave and millimeter-wave opacity of gaseous sulfur dioxide (SO_2) under simulated conditions for the Venus atmosphere, *Icarus*, 97, 200-210, 1992.

Gelman, B. G., V. G. Zolotukhin, L. M. Mukhin, N. I. Lamonov, B. V. Levchuk, D. F. Nenarokov, B. P. Okhotnikov, V. A. Rotin, and A. N. Lipatov, Gas chromatograph analysis of the chemical composition of the Venus atmosphere, *Space Res., 20*, 219, 1979.

Gross, E. P., Shape of collision-broadened spectral lines, *Phys. Rev., 97*, 395-403, 1955.

Hewlett-Packard Corporation, Hewlett-Packard Manual for the HP 8562A/B, pp. 1-20, California, 1989.

Ho, W., I. A. Kaufman, and P. Thaddeus, Laboratory measurement of microwave absorption in models of the atmosphere of Venus, *J. Geophys. Res., 71*, 5091-5108, 1966.

Janssen, M. A., and R. L. Poynter, The microwave absorption of SO_2 in the Venus atmosphere, *Icarus, 46*, 51-57, 1981.

Jenkins, J. M., P. G. Steffes, D. P. Hinson, J. D. Twicken, and G. L. Tyler, Radio occultation studies of the Venus atmosphere with the Magellan spacecraft, II, Results from the October 1991 experiments, *Icarus, 110*, 79-94, 1994.

Kolbe, W. F., B. Leskovar, and H. Buscher, Absorption coefficients of sulfur dioxide microwave rotational lines, *J. Mol. Spectrosc., 59*, 86-95, 1976.

Kreyszig, E., *Advanced Engineering Mathematics*, pp. 947-956, John Wiley, New York, 1983.

Krishnaji, and S. Chandra, Molecular interactions and line - widths of the asymmetric molecule SO_2, II, SO_2-CO_2 collisions, *J. Chem. Phys., 38*, 1019-1021, 1963.

Matthael, G. L., L. Young, and E. Jones, *Microwave Filters, Impedance-Matching Networks and Coupling Structures*, pp. 651-668, McGraw-Hill, New York, 1980.

Muhleman, D. O., G. S. Orton, and G. L. Berge, A model of the Venus atmosphere from radio, radar, and occultation observations, *Astrophys. J., 234*, 733-745, 1979.

Na, C. Y., L. W. Esposito, W. E. McClintock, and C. A. Barth, Sulfur dioxide in the atmosphere of Venus, II, Modeling results, *Icarus, 112*, 389-395, 1994.

Oyama, V. I., G. C. Carle, F. Woeller, J. B. Pollack, R. T. Reynolds, and R. A. Craig, Pioneer Venus gas chromatography of the lower atmosphere of Venus, *J. Geophys. Res., 85*, 7891-7902, 1980.

Pettengill, G. H., P. G. Ford, and R. J. Wilt, Venus surface radiothermal emission as observed by Magellan, *J. Geophys. Res., 97*, 13,091-13,102, 1992.

Poynter, R. L., and H. M. Pickett, Submillimeter, millimeter, and microwave spectral line catalog, *Appl. Opt., 24*, 2235-2240, 1985.

Ramo, S., J. R. Whinnery, and T. Van Duser, *Fields and Waves in Communication Electronics*, 2nd ed., pp. 279-281, John Wiley, New York, 1965.

Seiff, A., B. D. Kink, R. E. Young, R. C. Blanchard, J. T. Findlay, G. M. Kelly, and S. C. Sommer, Measurements of thermal structure and thermal contrasts in the atmosphere of Venus and related dynamical observation: Results from the four Pioneer Venus probes, *J. Geophys. Res., 85*, 7903-7933, 1980.

Spilker, T. R., New laboratory measurements on ammonia's inversion spectrum with implications for planetary atmospheres, *J. Geophys. Res., 98*, 5539-5548, 1993.

Steffes, P. G., and V. R. Eshleman, Laboratory measurements of the microwave opacity of sulfur dioxide and

other cloud-related gases under simulated conditions for the middle atmosphere of Venus, *Icarus*, *48*, 180-187, 1981.

Steffes, P. G., M. J. Klein, and J. M. Jenkins, Observations of the microwave emission of Venus from 1.3 to 3.6 cm, *Icarus*, *84*, 83-92, 1990.

Townes, C. H., and A. L. Schawlow, *Microwave Spectroscopy*, pp. 435-441, Dover, New York, 1955.

Van Vleck, J. H., and V. F. Weisskopf, On the shape of collision-broadened lines, *Rev. Mod. Phys.*, *17*, 227-236, 1945.

M. A. Kolodner, School of Physics, Georgia Institute of Technology, Atlanta, GA 30332-0430. (e-mail: gt8712a@prism.gatech.edu)

P. G. Steffes and S. H. Suleiman, School of Electrical and Computer Engineering, Georgia Institute of Technology, Atlanta, GA 30332-0250. (e-mail: paul.steffes@ee.gatech.edu; gt8835c@prism.gatech.edu)

(Received April 4, 1995; revised November 30, 1995; accepted December 5, 1995.)